

Particle swarm optimization for the estimation of surface complexation constants with the geochemical model PHREEQC-3.1.2

Ramadan Abdelaziz^{1,2}, Broder J. Merkel², Mauricio Zambrano-Bigiarini³, Sreejesh Nair⁴

¹ *College Of Engineering, A'Sharqiyah University, Oman*

² *TU Bergakademie Freiberg, Germany*

³ *Department of Civil Engineering, Universidad de La Frontera, Chile*

⁴ *Institute of Environmental Physics, University of Bremen, Germany*

Email: ramawaad@gmail.com, ramadan.abdelaziz@asu.edu.om

Abstract

Recently, Particle Swarm Optimization (PSO) techniques have attracted many researchers to optimize model parameters in several fields of research. This paper explains, for the first time, how to interface the hydroPSO R optimization package with the PHREEQC geochemical model, version 3.1.2. Sorption of metals on minerals is a key process in treatment water, natural aquatic environments, and other water related technologies. Sorption processes can be simulated by means of surface complexation models. However, determining thermodynamic constants for surface species from batch experiments requires a robust parameter estimation tool that does not get stuck in local minima. In this work, uranium at low concentrations was sorbed on quartz at different pH. Results show that hydroPSO delivers more reliable thermodynamic parameter values than **parameter estimation (PEST) software** when both are coupled to PHREEQC using the same thermodynamic input data. Post-processing tools included in hydroPSO are helpful for the interpretation of the results. Thus, hydroPSO is a recommended optimization tool for PHREEQC with respect to inverse modeling to determine reliable and meaningful thermodynamic parameter values.

Keywords: particle swam optimization; hydroPSO; PHREEQC; surface complexation; uranium; sorption

Introduction and Scope

The Particle Swarm Optimization technique (PSO) is an evolutionary optimization approach proposed by Eberhart and Kennedy (1995) and was influenced by the activities of flocks of birds in search of corn (Kennedy and Eberhart, 1995; Eberhart and Kennedy, 1995). Both PSO and genetic algorithms (GA)

28 shares a few similarities (Eberhart and Shi, 1998). GA **have** evolutionary operators like crossover or
29 selection while PSO does not have it (Eberhart and Shi, 1998). Recently, PSO has been implemented in a
30 wide range of applications, e.g. in the water resources (**Zambrano-Bigiarini and Rojas, 2013; Abdelaziz**
31 **and Zambrano-Bigiarini, 2014**), geothermal resources (Ma et al., 2013; Beck et al., 2010), finance and
32 economics (Das, 2012), in structural design (**Kaveh and Talatahari, 2009; Schutte and Groenwold, 2003**),
33 economics and finance (Huang et al., 2006; Das, 2012), and applications of video and image analysis
34 (Donelli and Massa, 2005; Huang and Mohan, 2007). For example, the groundwater model
35 MODFLOW2000/2005 was linked with PSO to estimate permeability coefficients (Sedki and Ouazar,
36 2010) and a multi-objective PSO code was used to **derive rainfall runoff** model parameters **by introducing**
37 **the Pareto rank concept** (Gill et al., 2006). **Notwithstanding recent popularity, PSO has never been** used to
38 calculate the parameters of a surface complexation model (SCMs) simulating sorption behavior of metal
39 and metalloids on mineral surfaces. Hence, this paper attempts to examine the efficiency and effectiveness
40 of PSO for parameter estimation of a surface complexation model as is PHREEQC (Parkhurst and Appelo,
41 1999).

42 Nowadays, a number of PSO software codes exist such as MADS (Harp and Vesselinov, 2011; Vesselinov
43 and Harp, 2012) and OSTRICH (Matott, 2005), with most of the codes using the basic PSO formulation
44 developed in 1995. However, in this paper we use the latest Standard Particle Swarm Optimization
45 proposed in literature (Clerk, 2012; Zambrano-Bigiarini et al., 2013), named SPSO2011, as implemented
46 in the *hydroPSO* R package (R Core team, 2016) version 0.3-3 (Zambrano-Bigiarini and Rojas, 2013;
47 2014). *hydroPSO* is an independent R package that includes the newest Standard PSO (SPSO-2011) ,
48 which was specifically developed to calibrate a wide range of environmental models. In addition, the
49 plotting functions in *hydroPSO* are user-friendly and aid the numeric and visual interpretation of the
50 optimization results. The source code, installation files, tutorial (vignette), and manual **are available** on
51 <http://cran.r-project.org/web/packages/hydroPSO>.

52

53 *hydroPSO* is used in this paper, for the first time, to estimate the parameters of a surface complexation for
54 U(VI)-Quartz system, to properly capture the non-linear interactions between the model parameters. The
55 aim of this article is to examine the **suitability** of *hydroPSO* as a global optimisation tool for parameter
56 estimation of geochemical models, in particular PHREEQC -3.1.2. **To this end, surface/sorption reaction**
57 **constants (log K) of the surface complexation model (SCM) obtained with hydroPSO will be compared to**
58 **those previously obtained with PEST (Doherty, 2010) by Nair et al. (2014).**

59 **Model description**

60 PHREEQC **version 3.1.2** (Parkhurst and Appelo, 1999), the database of Nuclear Energy Agency
61 thermodynamic NEA_2007 (Grenthe et al., 2007), as well as the LLNL database (Lawrence Livermore
62 National Laboratory) **are used to model sorption**. Both databases were modified by set constant values for
63 $\text{MUO}_2(\text{CO}_3)_3^{2-}$ and $\text{M}_2\text{UO}_2(\text{CO}_3)_3^0$ species (M equals Ca, Mg, Sr) taken from Geipel et al.(2008) and
64 Dong and Brooks (2006, 2008). PHREEQC is a geochemical code which is capable to simulate sorption,
65 surface complexation, and other types of reactions. SCMs are considered to be suitable tools to describe
66 the processes at liquid-solid interfaces (Huber and Lützenkirchen, 2009). Surface Complexation
67 Modelling (SCM) has been widely employed to **simulate the sorption of metal species** from aqueous
68 solution depending on solution concentration and pH value as well as ionic strength and redox conditions
69 (Davis et al., 2004; Štamberg et al., 2003; Zheng et al., 2003). **A group of reactions of aqueous species**
70 **from the bulk solution with the surface of the sorbent leads to the formation of surface complexes. The**
71 **constants for these reactions (surface complexation constants, log K) are indispensable for SCM.**

72 There are different SCMs like generalized two layer model (GTLM), nonelectrostatic model (NEM),
73 constant capacitance model (CCM), diffuse-layer model (DLM), modified triple-layer model (modified
74 TLM). Here, a generalized two layer model (GTLM) (Dzombak and Morel, 1990) was used to simulate
75 the sorption behavior of U(VI) on quartz. The GTLM was used instead of other models because it is
76 relatively simple and can be used in a wide range of chemical conditions. A comprehensive review of
77 GTLM is presented in Dzombak and Morel (1990). Quartz is a nonporous mineral and non-layered, and

78 therefore, the actual area of surface is supposed to be equal to the specific surface area. In this study, the
79 surface of quartz is considered as a single binding site **which takes the charge** for every surface reaction.
80 The sorption reactions and log K values are related to the aqueous species and thus depend on the
81 thermodynamic database used. Uranyl carbonate complexes— $(\text{UO}_2)_2\text{CO}_3(\text{OH})_3^-$, $\text{UO}_2(\text{CO}_3)_2^{2-}$ and
82 $\text{UO}_2(\text{CO}_3)_3^{4-}$ —are the dominant species under our experimental conditions. Therefore, the surface-
83 complexation reactions for quartz were calculated **with respect to these species**.
84 The sorption of U(VI) on quartz **was investigated** and discussed by (Huber and Lützenkirchen, 2009).
85 However, formation of Mg-, Ca-, and Sr–Uranyl-Carbonate **complexes shows a significant impact on the**
86 **sorption** of uranium on quartz. This was studied by Nair and Merkel (2011) in batch experiments adding
87 10 g of powdered quartz to 0.1 liter of water containing rather low U(VI) concentrations (0.126×10^{-6} M)
88 in the absence and **presence** of Mg, Sr, and Ca (1 mM) at a pH value between 9 and 6.5 in steps of 0.5.
89 NaHCO_3 (1×10^{-3} M) and NaCl (1.5×10^{-3} M) were used as ionic-strength buffers. The low U-
90 concentrations were used to avoid precipitation of Ca-U-carbonates. In the **absence** of alkaline earth
91 elements, the percentage of uranium was sorbed on quartz ca. 90% independent from pH. In the existence
92 of Mg, Sr, and Ca, the percentage of sorption of uranium on quartz declined to 50, 30, and 10%,
93 correspondingly (Nair and Merkel, 2011).
94 Table 1 displays the parameter ranges used to optimize the 6 parameters selected to calibrate PHREEQC,
95 based on Nair et al., 2014.

96 **Table 1: Complexation reactions with their respective log K range values.**

Corresponding Reaction	ID	Parameter Range values		Calibrated Parameter log K
		Min	Max	
$\text{Q}_x\text{OH} + \text{UO}_2(\text{CO}_3)_3^{4-} + \text{OH}^- \rightleftharpoons \text{Q}_x\text{OUO}_2(\text{CO}_3)_3^{5-} + \text{H}_2\text{O}$	K1	24	26	25.156
$\text{Q}_x\text{OH} + \text{UO}_2(\text{CO}_3)_2^{2-} + \text{OH}^- \rightleftharpoons$	K2	20	23	21.18

$Q_xOUO_2(CO_3)_2^{3-} + H_2O$				
$Q_xOH + UO_2CO_3 \rightleftharpoons Q_xOUO_2CO_3^- + H^+$	K3	-8	-5	-5.589
$Q_xOH + UO_2OH^+ \rightleftharpoons Q_xOUO_2OH + H^+$	K4	2	4	3.229
$Q_xOH + (UO_2)_2CO_3(OH)_3^- \rightleftharpoons Q_xO(UO_2)_2CO_3(OH)_3^{2-} + H^+$	K5	5	8	6.733
$Q_xOH + Na^+ \rightleftharpoons Q_xONa + H^+$	K6	-7	-4	-5.842

Q_xOH: Silanol surface site

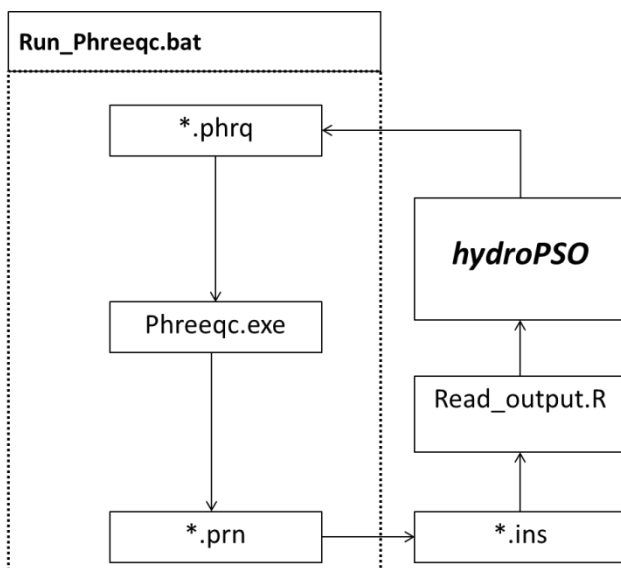
97

98 Computational implementation

99 Inverse modeling is a complex issue for modelers as a result of the numerous uncertainties in model
100 parameters and observations (e.g., Carrera et al., 2005; Beven, 2006). Particle Swarm Optimisation (PSO)
101 is an evolutionary optimisation algorithm originally developed by Kennedy and Eberhart (1995), which
102 has proven to be highly efficient when solving a large collection of case studies from different disciplines
103 (see, e.g., Poli, 2008). In PSO each individual of the population searches for the global optimum in a
104 multidimensional parameter space, considering the individual and collective past experiences. The
105 canonical PSO algorithm starts with a random initialization of the particles' positions and velocities within
106 the multi-dimensional parameter space. Velocity and position of each particle in the parameter space are
107 updated in successive iterations following equations specific to the selected PSO version, trying to find the
108 minimum (or maximum) of a user-defined objective function (see a complete description in Zambrano-
109 Bigiarini and Rojas, 2013). In the last decades, several improvements have been proposed to the canonical
110 PSO algorithm, and hydroPSO implements several of them in a single piece of software. In particular,
111 hydroPSO implements six PSO variants (equations used to update particles' position and velocities), four
112 different topologies (wa), two different initialization of particles' positions (random uniform distribution or
113 Latin Hypercube Sampling), five different alternatives for initializing particles' velocities, among many
114 other fine-tuning options (see Zambrano-Bigiarini and Rojas, 2013). In the application of hydroPSO to

115 PHREEQC, the following configuration was used: a swarm with 10 particles, 200 iterations, LH
116 initialisation of particle positions and velocities, random topology with 11 informants, acceleration
117 coefficients c_1 and c_2 equal to 2.05, linearly decreasing clamping factor for V_{max} in the range [1.0, 0.5],
118 and use of the Clerc's constriction factor instead of the inertia weight. The hydroPSO R package v0.3-3
119 (Rojas and Zambrano-Bigiarini, 2012; Zambrano-Bigiarini and Rojas, 2013; 2014) is a model-independent
120 optimization package, which implements a state-of-the-art PSO algorithm to carry out a global parameter
121 optimisation, and it has been successfully applied as calibration tool for both hydrogeological and
122 hydrological models (Zambrano-Bigiarini and Rojas, 2013; Thiemig et al., 2013; Abdelaziz and
123 Zambrano-Bigiarini, 2014; Bisselink et al., 2016), requiring no instruction or template files as UCODE
124 (Poeter et al., 2005; Abdelaziz and Merkel, 2015) and PEST software (Doherty, 2005; 2013) do. In order
125 to couple *hydroPSO* with the PHREEQC geochemical model, three text files have to be prepared by the
126 user to handle data transfer between the model code and the optimization engine: (i) '*ParamFiles.txt*',
127 which describes the names of a set of parameters to be estimated and locations in the model input files to
128 be utilized in the inverse procedure, (ii) '*ParamRanges.txt*', which defines the minimum and maximum
129 values that each selected parameter might have during the optimization, and (iii) '*PSO_OBS.txt*', which
130 contains the observations that will be compared against its simulated counterparts. In addition, a user-
131 defined R script file ('*Read_output.R*') have to be prepared, containing the instructions to read model
132 outputs, while an R script template provided by hydroPSO (Rojas and Zambrano-Bigiarini, 2012) has to
133 be slightly modified by the user in order to carry out the optimization. In contrast to coupling PEST with
134 PHREEQC **is** required to run PEST with PHREEQC. The four files were required: i) template files (*.tpl),
135 ii) instruction files (*.ins), iii) a main control file (*.pst), and iv) a batch file to execute PHREEQC and
136 PEST(*.bat) . Template files **are** built to modify the input files for PHREEQC with other values while an
137 instruction file **is** employed to extract the simulated values from the output file for PHREEQC. The main
138 control file includes a model application will be run, the observations, parameters to be estimated, control
139 data keywords, and etc. For further information about PEST read the manual is recommended. However,
140 Figure 1 shows the key files used to couple PHREEQC with hydroPSO, and explains the flowchart and

141 files involved in the inverse modelling of the surface complexation constants for the U(VI) sorption
 142 model.



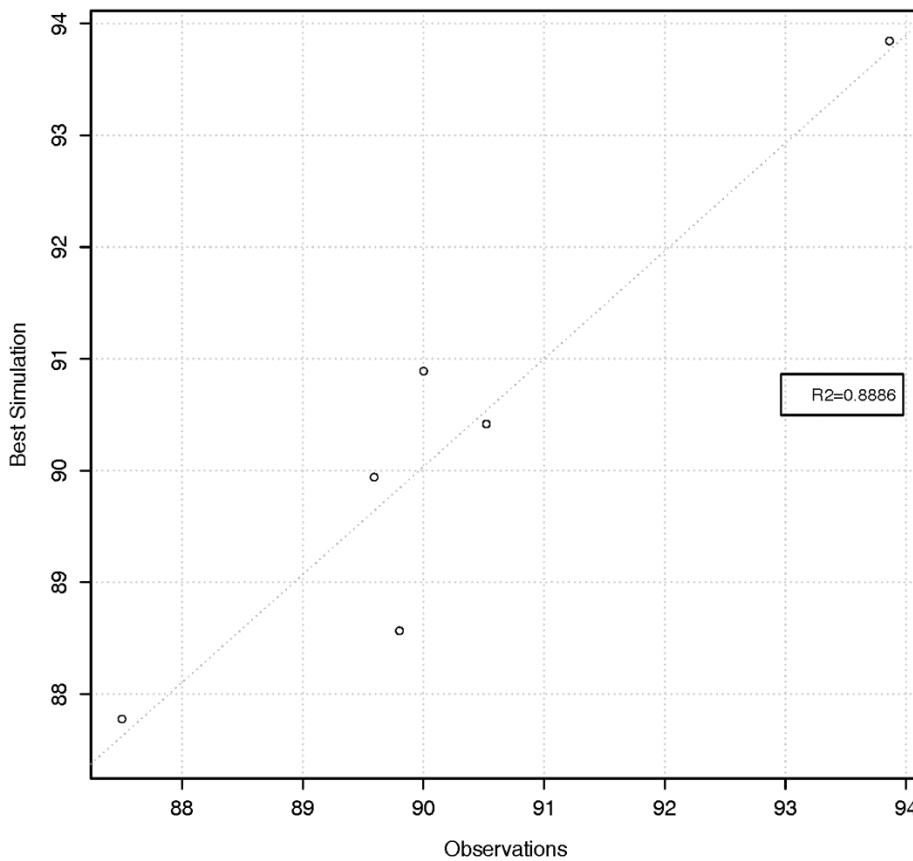
143
 144 **Figure 1: Flow chart with files involved in inverse modeling of surface complexation constants for**
 145 **uranium carbonate (U(VI)) species on quartz with the PHREEQC geochemical model.**

146 For numerical optimization, the residual sum of squares (RSS or SSR, see Equation (1)) was utilized to
 147 compute the goodness of fit (*GoF*) between the corresponding model outputs (C_j^s) and observed U-
 148 carbonate concentration values (C_j^o) at different pH values for every iteration step i . After some initial
 149 trials, the number of maximum iterations T was set to 200 and the number of particles used to search for
 150 the minimum RSS in the parameter space was fixed at 10 (i.e., 2000 runs of the model). The rest of
 151 parameters were set to the default values defined in hydroPSO. More information about SPSO 2011 can
 152 be found in Clerc (2012), Zambrano-Bigiarini et. al. (2013), while detailed information about hydroPSO
 153 can be found in Zambrano-Bigiarini and Rojas (2013). All the input files required for running PHREEQC
 154 and hydroPSO can be found in the supplementary material
 155 (<https://zenodo.org/record/1044951#.WgVTbVuCzIU>), including all the optimization results.

$$SSR = \sum_{i=1}^n (C_j^s - C_j^o)^2 \quad (1)$$

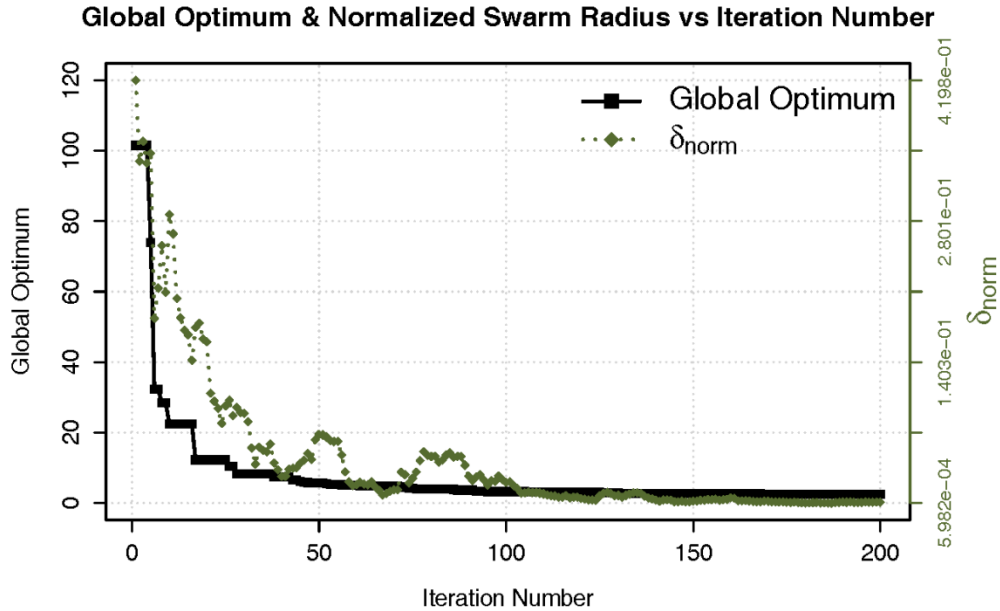
156 **Results and Discussion**

157 One of the vital and useful approaches to evaluate the efficacy of model performance is through
158 plotting the simulation against observed values (visualizing outcome of model). **The observed and**
159 **simulated** sorption ratio and the calculated sorption ratio **are compared in Figure 2.** The coefficient of
160 determination (R2) for the relation between calculated and observed values is 0.89, indicating a high linear
161 correlation and thus high model quality (Figure 2).



162

163 **Figure 2: Scatter plot with the experimentally observed and calculated values of uranium carbonate**
164 **(sorption %).**



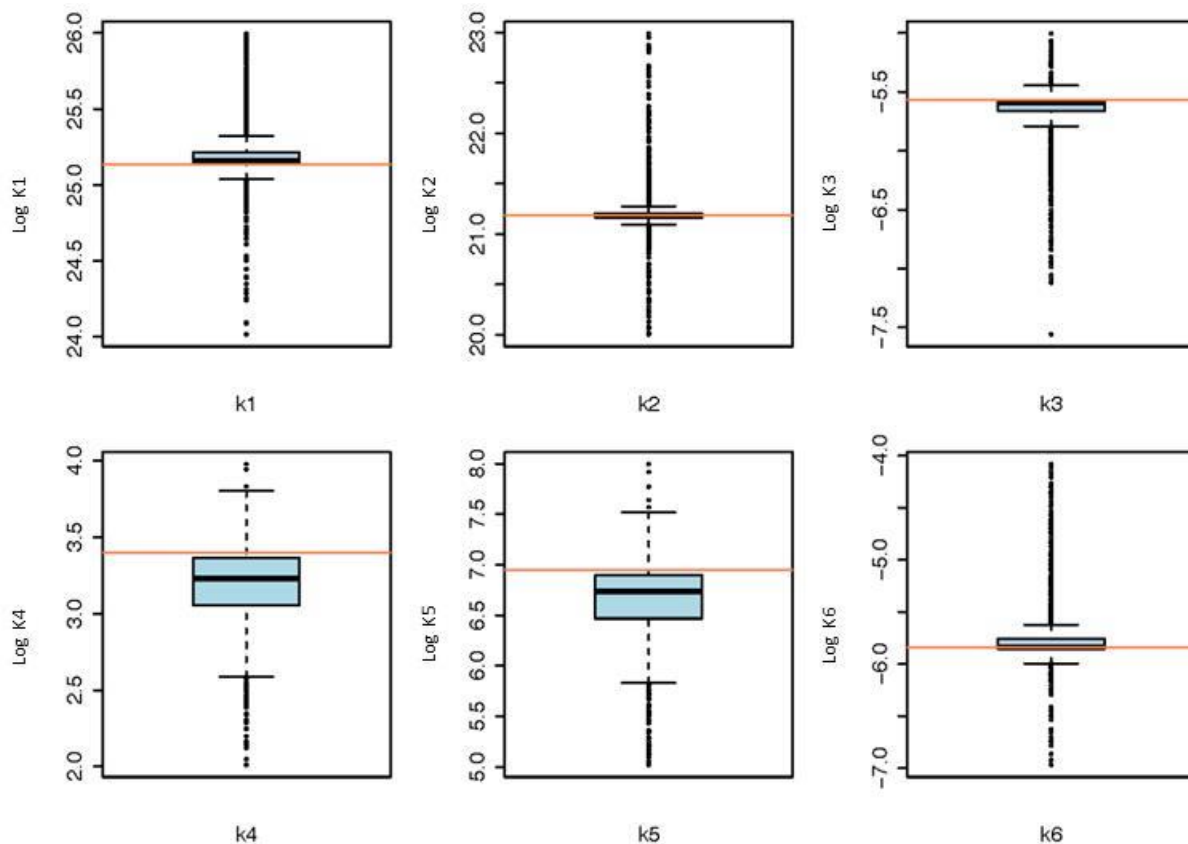
165

166 **Figure 3: Evolution of the normalized swarm radius (δ norm) and the global optimum (SSR) over**
 167 **200 iterations.**

168 However In hydroPSO there are two types of criteria for convergence: i) **absolute**, when the global
 169 optimum found in a given iteration is below/above than a user-defined threshold (useful for
 170 minimization/maximization problems where the true minimum/maximum is known); ii) **relative**, when
 171 the absolute difference between the model performance in the current iteration and the model
 172 performance in the previous iteration for the best performing particle is less or equal to a user-defined
 173 threshold (useful to prevent too many model runs without any improvement in the optimum found by the
 174 algorithm). If none of the two previous criteria are met, then the algorithm stops when the user-defined
 175 number of iterations is finally achieved. Figure 3 shows the evolution of the best model performance (i.e.,
 176 smallest RSS) found by all the particles in a given iteration, and the normalized swarm radius (δ_{norm} , a
 177 measure of the spread of the population in the range of search-space) versus the iterations number. One
 178 may observe that both δ_{norm} and the best model performance become smaller with an increasing iteration
 179 number, which indicates that the main particles are “flying” around a small region in parameter space,
 180 Only 100 iterations (i.e., $100 \times 10 = 1000$ model runs) were enough to reach the region of the global

181 optimum (i.e, RSS ca. 2.52), and the remaining iterations were just used to refine the search as shown in
182 Figure 3.

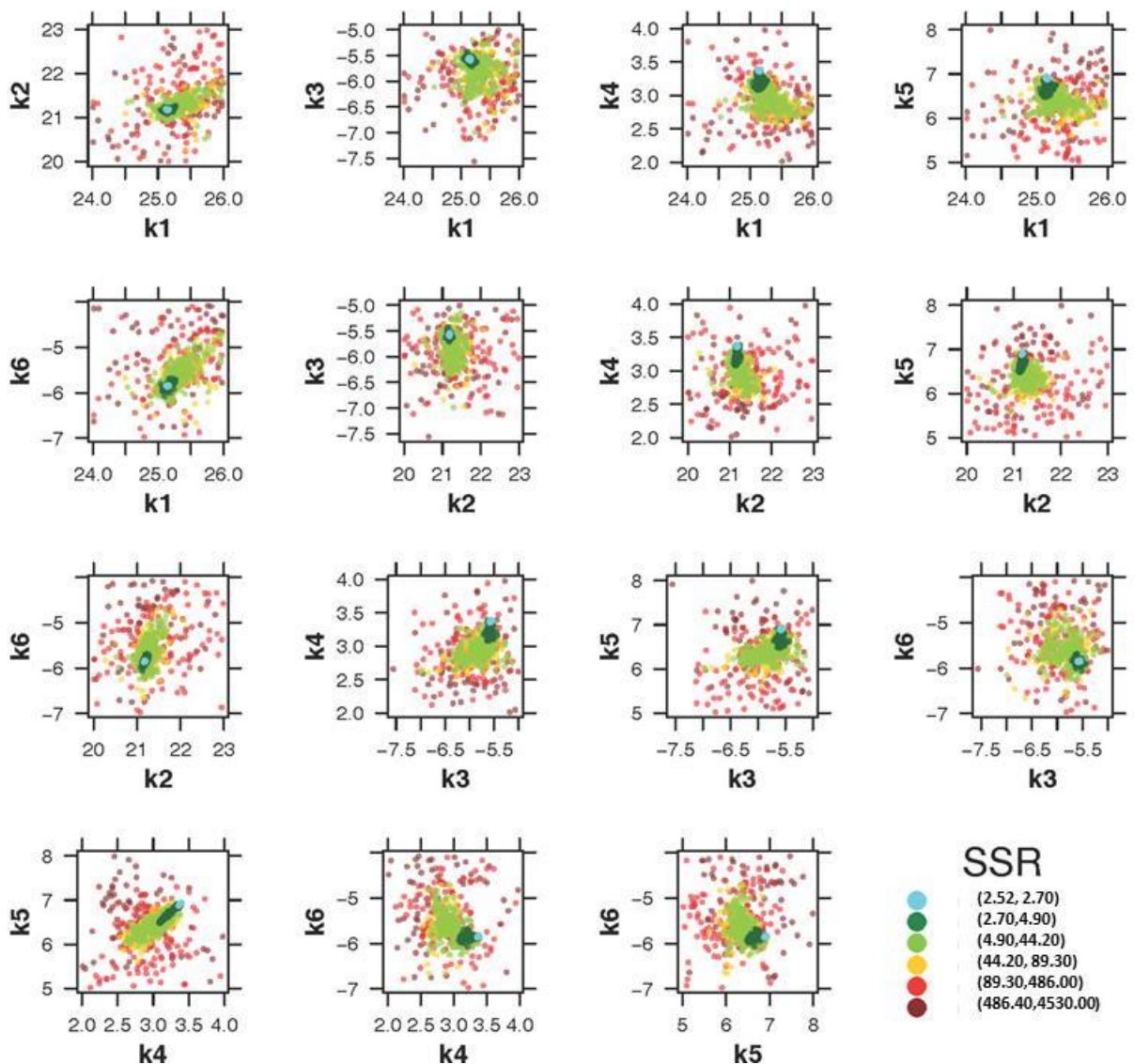
183 The boxplots in Figure 4 are graphical representations of the values sampled during optimization. The
184 bottom and top of the box show the first and third quartiles of the distribution of each one of the
185 surface/sorption reaction constants(log K) sampled during the optimization, respectively. The horizontal
186 line within the box denotes the median of the distribution. Points outside the whiskers are considered to be
187 outliers, where notches are within $\pm 1.58IQR/\sqrt{n}$, IQR represents the interquartile range and n the total
188 number of parameter sets used in the optimization. The horizontal red lines in Figure 4 point out the
189 optimum value found during optimization for each parameter.



190
191 Figure 4: Boxplots for the optimised parameters. The horizontal red lines indicate the optimum
192 value for each parameter. Parameter names are defined in Table 1.

193 Two dimensional dotted plots in Figure 5 depict the goodness-of-fit values achieved by different
194 parameter sets. They are suitable for identifying ranges where different sets of parameters lead to the same
195 model performance (equifinality, Beven , 2006).

196 Figure 5 shows the model performance as function of the interaction of different parameter ranges.
197 The (quasi) three-dimensional dotted plot shown in Figure 5 is a projection of the values of pairs of
198 parameters onto the model response surface “RSS”. Parameter values where the model presents high
199 performance are shown in light-blue (points density), whilst the parameter values where the model shows
200 low performance are shown in dark-red (points density). This figure was used to identify regions of the
201 solution space with good and bad model performances (Figure 5).



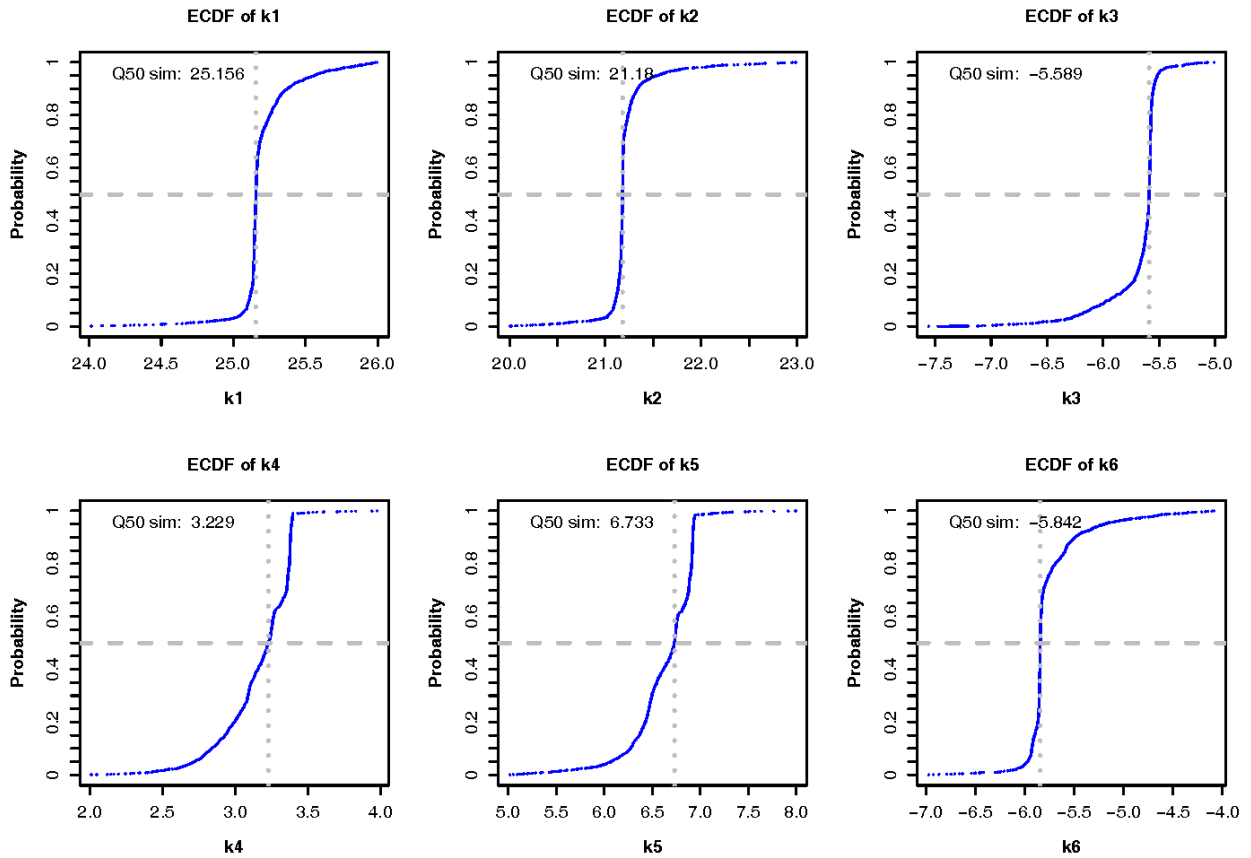
202

203 **Figure 5: Quasi three-dimensional dotted plots.**

204 Visual inspection of Figure 5 shows a good exploratory capability of PSO because the particles are
 205 well spread over the entire range space. It is clearly visible that the parameter samples are denser around
 206 the optimum value (lowest SSR), showing a small uncertainty range around the optimum value.

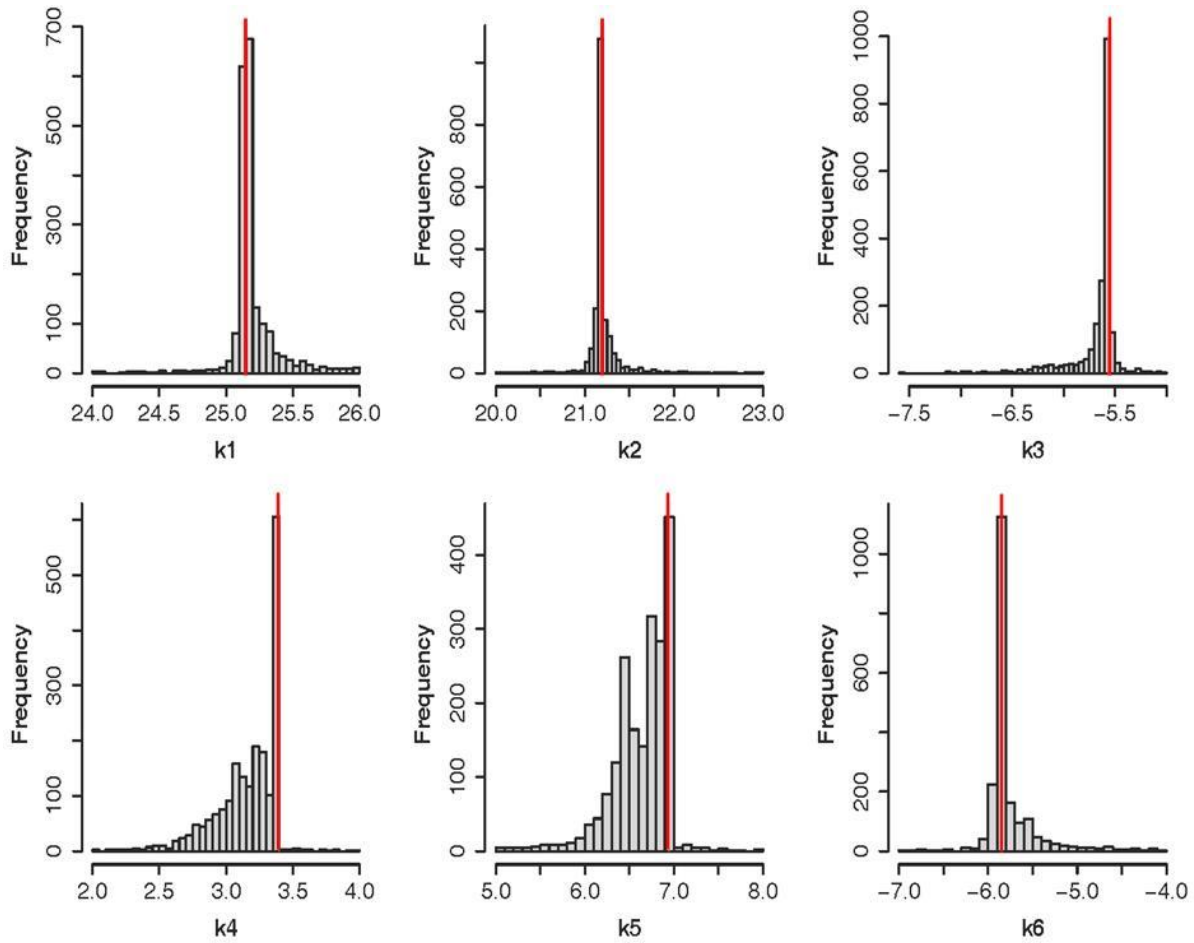
207 Figure 6 and Figure 7 give a graphical summary for optimised parameters. Empirical Cumulative
 208 Density Functions (ECDF) in Figure 6 shows the sampled frequencies for the six calibrated parameters.
 209 The horizontal gray dotted lines show the median of the distribution (cumulative probability equal to 0.5)
 210 whiles the vertical gray dotted lines depict the corresponding parameter value, display at the top of every

211 figure (Figure 6). The thin vertical red line in Figure 7 points out the optimum value achieved for each
212 parameter. Histograms in figure 7 show near-normal distributions for K1 and K2, while k4 and k5 follow
213 a skewed distribution with sampled values concentrated near the upper boundary of each parameter.



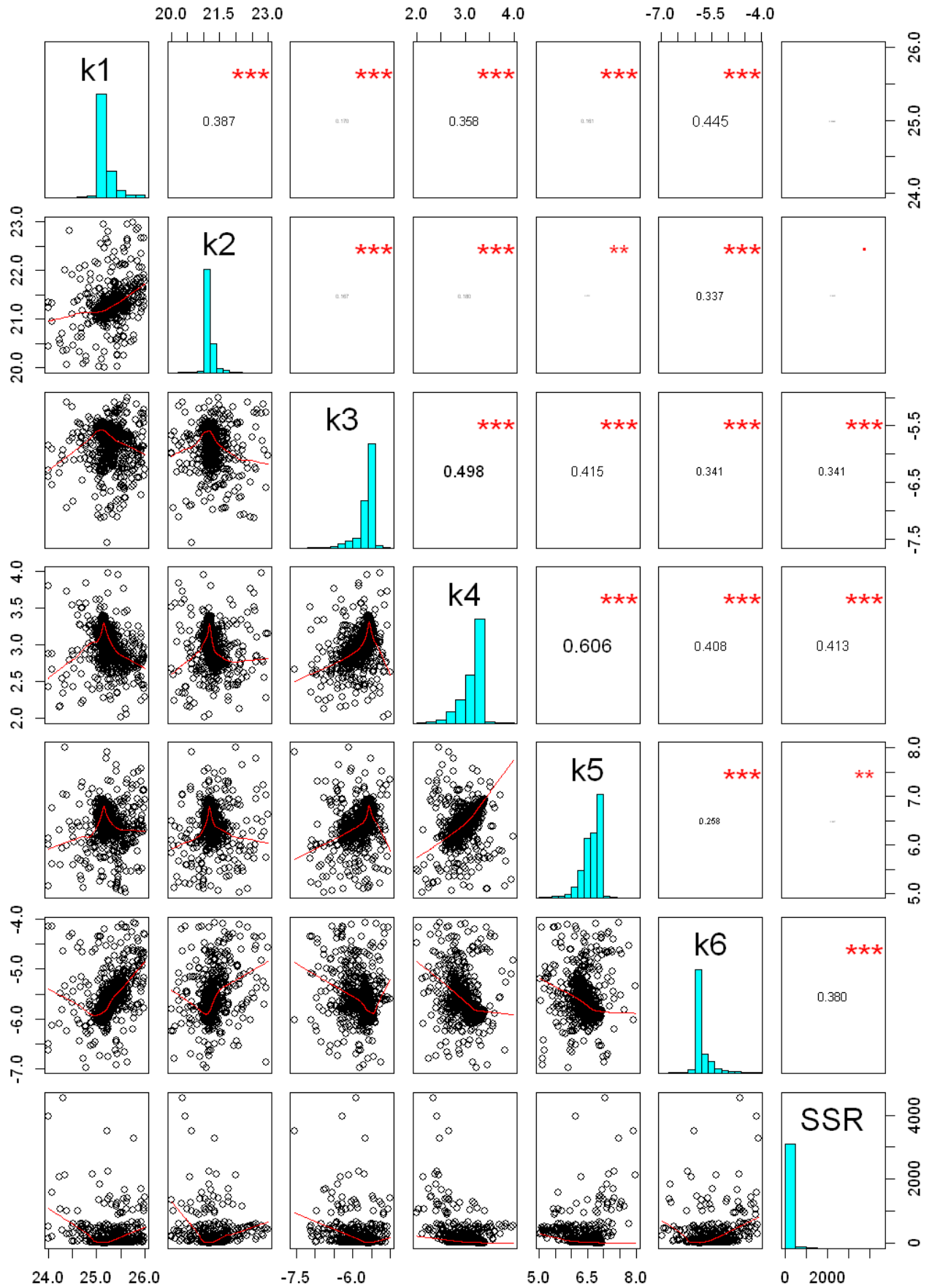
214

215 **Figure 6: Empirical cumulative density functions for each calibrated parameter.**

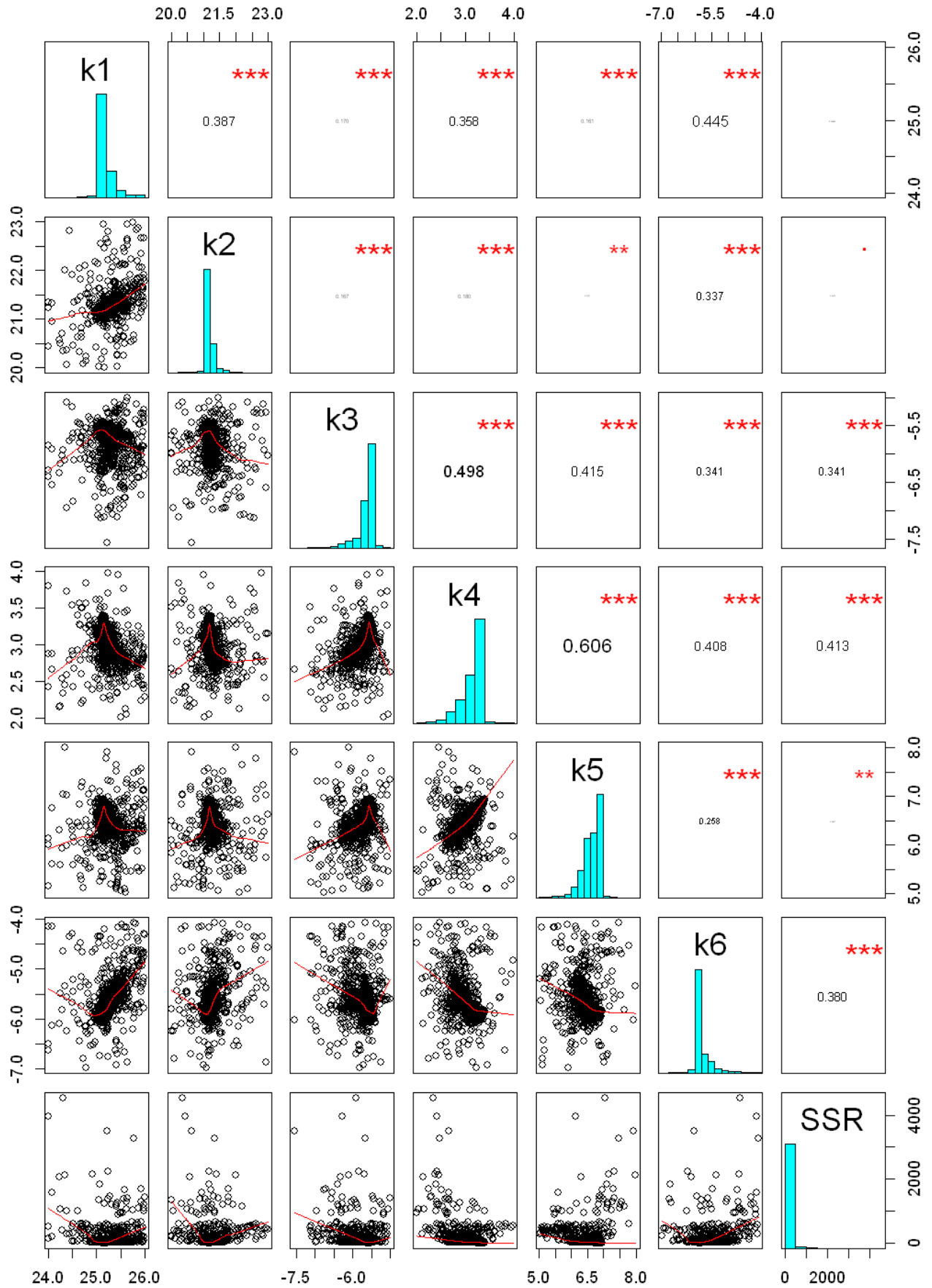


216

217 **Figure 7: Histograms of calibrated parameter values. Horizontal axis shows the sampled range for**
 218 **each parameter and vertical axis represents the amount of parameter sets in each of the classes used**
 219 **to divide the horizontal axis.**

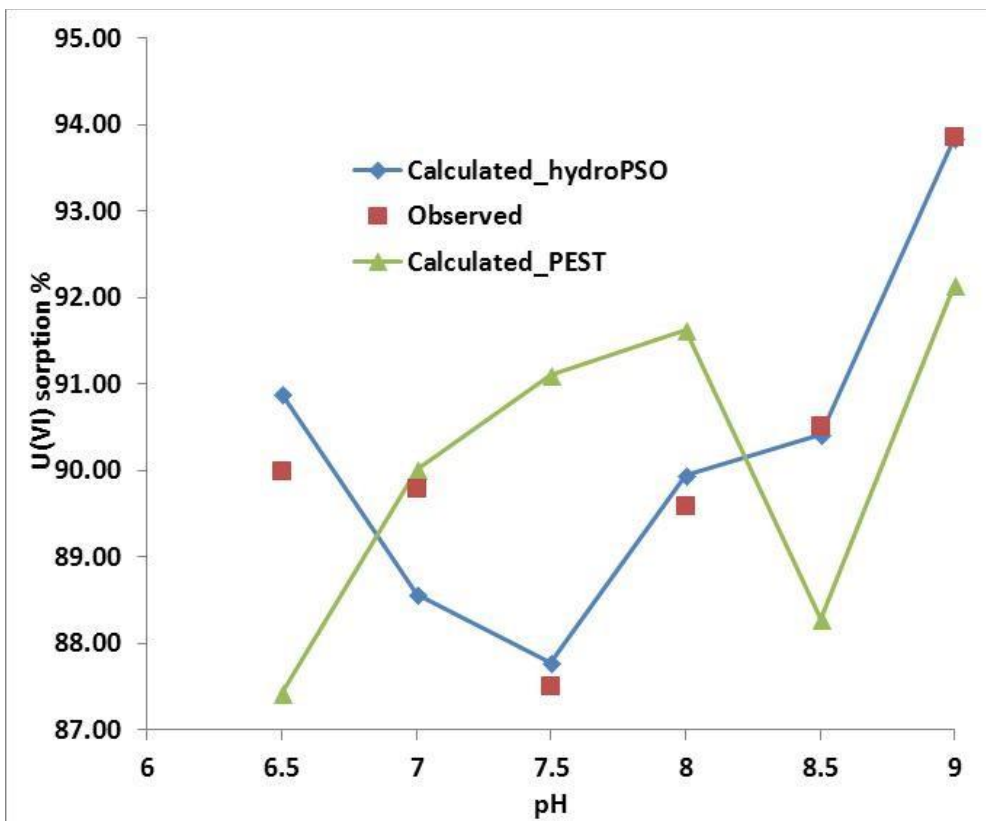


222 **Figure 8** illustrates the correlation matrix among K values and model performance (SSR), with horizontal
223 and vertical axes displaying the ranges used for the calibration of each parameter. The figure represents
224 that highest correlation coefficient occurred among the measure of model performance (SSR) and K4, K6,
225 and K3. In addition, a higher correlation coefficient was observed between K4 and K5, K3 and K4, and
226 K1 and K6.



228 **Figure 8: Correlation matrix between model performance (SSR) and calibrated parameters.**
 229 **Red lines represents lowess smoothing, using locally-weighted polynomial regression, and numbers**
 230 **in the upper panel represents the Pearson-moment correlation coefficient between each pair of**
 231 **parameters. Vertical and horizontal axes illustrate the physical range utilized for parameter**
 232 **optimization. *** stands for a $p < 0.001$; ** stands for $p < 0.01$, according to level of statistical**
 233 **significance**

234 Figure 9 shows the model output using hydroPSO fitted log-K values and the monitored sorption ratio.



235
 236 **Figure 9: Observed and simulated sorption of uranium in quartz vs pH with both PEST and**
 237 **hydroPSO calibrated log-k values.**

238 It is worthwhile to mention that the surface complexation constants for the equations 1, 2, and 5 are
 239 more important and the equations that are less important are 3, 4, and 6 in optimizing the “log K” values.
 240 It proves that $\text{UO}_2(\text{CO}_3)_3^{4-}$, $\text{UO}_2(\text{CO}_3)_2^{2-}$, and $(\text{UO}_2)\text{CO}_3(\text{OH})_3^-$ are the most dominate species sorption on
 241 quartz. From the optimized model, the surface complexation constants for the equations 2 and 4 was
 242 optimized to be 21.18 and 3.229 respectively (Nair et al., 2014), which is higher than the electrostatic (ES)

243 and nonelectrostatic (NES) models, while the optimized value for equation 1 is 25.156, which is higher
244 than the NES model and almost the same as the ES model (Nair et al., 2014).

245 Comparing the results of optimized log-K values for GTLM as sorption model which obtained by
246 hydroPSO versus previous work done by Nair et al. (2014). The experimental conditions and the
247 PHREEQC modelling assumptions were the same during the PEST optimisation. In other words, PEST
248 was applied for the similar case and the same data, we can show that the log k values obtained with
249 hydroPSO are better estimations than those obtained by PEST, except for pH=7. The main reason is that
250 PSO is a global optimization technique, which searches for optimum values in the parameter space as
251 defined by the ranges given in Table 1, while PEST searches on a neighborhood of the initial solution. In
252 particular, PEST carries out inverse modelling by computing value of parameters that minimize a
253 weighted least-squares objective function via the Gauss-Marquardt-Levenberg non-linear regression
254 method (Marquardt, 1963). Actually, a major drawback of PEST, as of all gradient-based techniques, is
255 the dependency of the quality of the optimization results upon the initial point used for the optimization,
256 which might lead to a local optimum rather than the global one. Thus, PSO techniques offer promising
257 possibilities for similar surface complexation and reactive transport applications in hydrogeology and
258 hydrochemistry.

259 **Conclusions**

260 The coupling of hydroPSO and PHREEQC was successfully carried to estimate surface complexation
261 constants for uranium (VI) species on quartz, based on a data set published by Nair and Merkel(2011), and
262 Nair et al.(2014). The open-source hydroPSO R package proved to be a useful tool for inverse modeling
263 of surface complexation models with PHREEQC and allowed a prompt evaluation of the calibration
264 results. Furthermore, thermodynamic values obtained with *hydroPSO* provided a better match to
265 observation sorption rates in comparison to those obtained with PEST, using the same input data.

266 **Data availability**

267 PHREEQC is available in the following <http://www.hydrochemistry.eu/ph3/index.html>. Source code,
268 tutorials, and reference manual of hydroPSO can be obtained from [https://CRAN.R-](https://CRAN.R-project.org/package=hydroPSO)
269 [project.org/package=hydroPSO](https://CRAN.R-project.org/package=hydroPSO). The PHREEQC model input files along with the R scripts used for
270 coupling it with hydroPSO and the model outputs can be obtained from the Zenodo repository
271 (<https://zenodo.org/record/1044951#.WgVTbVuCzIU>).

272 **References**

- 273 Abdelaziz, R.; ZAMBRANO-BIGIARINI, M. Particle Swarm Optimization for inverse modeling of solute
274 transport in fractured gneiss aquifer. *Journal of contaminant hydrology*, **2014**, 164. Jg., S. 285-298.
- 275 Abdelaziz, R.; Merkel, B.J., 2015. Sensitivity analysis of transport modeling in a fractured gneiss aquifer.
276 *Journal of African Earth Sciences*, 103, pp.121-127.
- 277 Beck, M.; Hecht-Méndez, J.; de Paly, M.; Bayer, P.; Blum, P.; Zell, A. Optimization of the energy
278 extraction of a shallow geothermal system. 2010 IEEE Congress on Evolutionary Computation (CEC),
279 **2010**, pp. 1–7.
- 280 Beven, K. **A manifesto for the equifinality thesis**. *Journal of hydrology*, **2006**, 320. Jg., Nr. 1, S. 18-36.
- 281 Bisselink, B., Zambrano-Bigiarini, M., Burek, P., & de Roo, A. (2016). Assessing the role of uncertain
282 precipitation estimates on the robustness of hydrological model parameters under highly variable climate
283 conditions. *Journal of Hydrology: Regional Studies*, 8, 112-129.
- 284 Clerc, M. Standard Particle Swarm Optimisation. Technical Re-port. Particle Swarm Central.
285 http://clerc.maurice.free.fr/ps/SPSO_descriptions.pdf. [Online. Last accessed 24-Sep-2012], **2012**.
- 286 Carrera, J; Alcolea, A.; Medina, A.; Hidalgo, J.; Slooten, L. J.. Inverse problem in hydrogeology.
287 *Hydrogeology journal*, **2005**, 13. Jg., Nr. 1, S. 206-222.
- 288 Das, Parichay. Economics of Distributed Generation Using Particle Swarm Optimization: A Case Study.
289 *Economics*, **2012**, 1. Jg., Nr. 5.
- 290 Davis, J.A.; Meece, DE, Kohler M, Curtis GP (2004) Approaches to surface complexation modeling of
291 uranium(VI) adsorption on aquifer sediments. *Geochimica Et Cosmochimica Acta*, **2004**,68 (18):3621-
292 364.1.
- 293 Doherty, J. PEST: model-independent parameter estimation, user manual. Technical Report (5th
294 ed.)Watermark Numerical Computing, Brisbane, Queensl., Australia, **2005**.
- 295 Doherty, J. PEST: Model-independent Parameter Estimation. User Manual, fifth ed. Watermark
296 Numerical Computing, **2010**.
- 297 Doherty, J. Addendum to the PEST manual. Technical Report Watermark Numerical Computing, Brisbane,
298 Queensl., Australia, **2013**.
- 299 Dong, W.M.; Brooks, S.C. Determination of the formation constants of ternary complexes of uranyl and
300 carbonate with alkaline earth metals (Mg^{2+} , Ca^{2+} , Sr^{2+} , and Ba^{2+}) using anion exchange method. *Environ*
301 *Sci Technol*, **2006**, 40:4689–4695.

302 Dong, W.M.; Brooks, S.C. Formation of aqueous $\text{MgUO}_2(\text{CO}_3)_3^{2-}$ complex and uranium anion exchange
303 mechanism onto an exchange resin. *Environ Sci Technol*, **2008**, 42:1979–1983.

304 Donelli, M., Massa, A. Computational approach based on a particle swarm optimizer for microwave
305 imaging of two-dimensional dielectric scatterers. *IEEE Transactions on Microwave Theory and*
306 *Techniques*, **2005**,53(5), 1761-1776.

307 Dzombak, D.A.; Morel, F.M. Surface complexation modeling: Hydrous ferric oxide. John Wiley & Sons,
308 New York, **1990**.

309 Eberhart, R.; Kennedy, J. A new optimizer using particle swarm theory. *Proceedings of the Sixth*
310 *International Symposium on Micro Machine and Human Science*, 1995. MHS'95, 1995,pp. 39–43.

311 Eberhart, R.C.; Shi, Y. Comparison between genetic algorithms and particle swarm optimization, in
312 *Evolutionary Programming VII*, V. Porto, N. Saravanan, D. Waagen, and A. Eiben, Eds. Springer Berlin /
313 Heidelberg, **1998**,vol. 1447, pp. 611–616. doi: 10.1007/BFb0040812.

314 Geipel, G.; Amayri, S.; Bernhard, G. Mixed complexes of alkaline earth uranyl carbonates: a laser-
315 induced time-resolved fluorescence spectroscopic study. *Spectrochimica Acta Part A-Mol Biomol*
316 *Spectrosc*, **2008**, 71:53–58.

317 Gill, M. K.; Kaheil, Y. H.; Khalil, A.; McKee, M.; Bastidas, L. Multiobjective particle swarm
318 optimization for parameter estimation in hydrology. *Water Resources Research*, **2006**,42(7).
319 doi:10.1029/2005WR004528.

320 Grenthe, I.; Fuger, J.; Konings R.; Lemire, R.J.; Muller, A.B.; Wanner, J. *The Chemical Thermodynamics*
321 *of Uranium*. Elsevier: New York, **2007**.

322 Harp, D., Vesselinov, V.V., Recent developments in MADS algorithms: ABAGUS and Squads, EES-16
323 Seminar Series, LA-UR-11-11957, **2011**.

324 Huang, F. Y.; Li, R. J.; Liu, H. X.; Li, R. A modified particle swarm algorithm combined with fuzzy
325 neural network with application to financial risk early warning. In *Services Computing*, 2006. APSCC'06.
326 *IEEE Asia-Pacific Conference*, IEEE, **2006**, 168-173.

327 Huang, T., & Mohan, A. S. A microparticle swarm optimizer for the reconstruction of microwave images.
328 *IEEE Transactions on Antennas and Propagation*, **2007**,55(3), 568-576.

329 Huber, F.; Lutzenkirchen, J., Uranyl Retention on Quartz-New Experimental Data and Blind Prediction
330 Using an Existing Surface Complexation Model. *Aquatic Geochemistry*, **2009**, 15, (3), 443-456.

331 Kaveh, A., Talatahari, S. A particle swarm ant colony optimization for truss structures with discrete
332 variables. *Journal of Constructional Steel Research*, **2009**,65(8), 1558-1568.

333 Kennedy, J.; Eberhart, R. Particle swarm optimization, in: *neural networks*, 1995. *Proceedings. IEEE*
334 *International Conference on Neural Networks*, **1995**, pp. 1942–1948.

335 Ma, R.J.; Yu, N.Y.; Hu, J.Y. Application of particle swarm optimization algorithm in the heating system
336 planning problem. *Sci. World J.* 11., **2013**, <http://dx.doi.org/10.1155/2013/718345>.

337 Marquardt, D. An algorithm for least-squares estimation of nonlinear parameters. *Journal of the Society*
338 *for Industrial and Applied Mathematics*, **1963**,11. pp. 431–441.

339 Matott, L. *Ostrich: An Optimization Software Tool, Documentation and User's Guide, Version 1.6.*
340 *Department of Civil, Structural and Environmental Engineering, University at Buffalo, Buffalo, NY,*
341 **2005**.

342 Nair, S.; Merkel B. J. Impact of Alkaline Earth Metals on Aqueous Speciation of Uranium(VI) and
343 Sorption on Quartz. *Aquatic Geochemistry*, **2011**,1 17 (3):209-219

344 Nair, Sreejesh; Karimzadeh, Lotfollah; Merkel, Broder J. Surface complexation modeling of Uranium
345 (VI) sorption on quartz in the presence and absence of alkaline earth metals. *Environmental Earth*
346 *Sciences*, **2014**, 71. Jg., Nr. 4, S. 1737-1745.

347 Parkhurst, D.L.; Appelo, C.A. User's Guide to PHREEQC (version 2). A Computer Program for
348 Speciation, Batch-Reaction, One-Dimensional Transport, and Inverse Geochemical Calculation. USGS,
349 Water Resources Investigation Report, **1999**, 99 – 4259.

350 Poli, R. Analysis of the publications on the applications of particle swarm optimisation. *Journal of*
351 *Artificial Evolution and Applications*, **2008**.

352 Poeter, E.; Hill, M.; Banta, E.; Mehl, S.; Christensen, S. UCODE 2005 and six other computer codes for
353 universal sensitivity analysis, calibration, and uncertainty evaluation. *US Geological Survey Techniques*
354 *and Methods*, **2005**, vol. 6-A11.

355 R Core Team. R: A Language and Environment for Statistical Computing. R Foundation for Statistical
356 Computing. Vienna, Austria. URL: <http://www.R-project.org/>, **2016**.

357 Rojas, R.; Zambrano-Bigiarini, M. Tutorial for interfacing hydroPSO with SWAT-2005 and MODFLOW-
358 2005. Technical Report. URL: http://www.rforge.net/hydroPSO/files/hydroPSO_vignette.pdf. [Online.
359 Last accessed 03-Feb-2014], **2012**.

360 Schutte, J. F., Groenwold, A. A. Sizing design of truss structures using particle swarms. *Structural and*
361 *Multidisciplinary Optimization*, **2003**, 25(4), 261-269.

362 Sedki, A.; Ouazar, D. Swarm intelligence for groundwater management optimization. *Journal of*
363 *Hydroinformatics*, **2011**,13(3), 520-532.

364 Štamberg, K.; Venkatesan, K. A.; Vasudeva Rao, P. R. Surface complexation modeling of uranyl ion
365 sorption on mesoporous silica. *Colloids and Surfaces A: Physicochemical and Engineering Aspects*, **2003**,
366 221. Jg., Nr. 1, S. 149-162.

367 Thiemig, V., Rojas, R., Zambrano-Bigiarini, M., De Roo, A. Hydrological evaluation of satellite-based
368 rainfall estimates over the Volta and Baro-Akobo Basin. *Journal of Hydrology*, **2013**,499, 324-338.

369 Vesselinov, V.V.; Harp, D.R. Adaptive hybrid optimization strategy for calibration and parameter
370 estimation of physical process models. *Computers & Geosciences*, **2012**, 49, 10–20.
371 doi:10.1016/j.cageo.2012.05.027.

372 Zambrano-Bigiarini, M.; Rojas, R. A model-independent Particle Swarm Optimisation software for model
373 calibration. *Environmental Modelling & Software*, **2013**, 43, 5-25. doi:10.1016/j.envsoft.2013.01.004.

374 Zambrano-Bigiarini, M.; Rojas, R. hydroPSO: Particle Swarm Optimisation, with focus on Environmental
375 Models. URL: <http://www.rforge.net/hydroTSM/>, <http://cran.r-project.org/web/packages/hydroTSM/> .R
376 package version 0.3-3, **2014**.

377 Zambrano-Bigiarini, M., Clerc, M., & Rojas, R. (2013, June). Standard particle swarm optimisation 2011 at cec-
378 2013: A baseline for future pso improvements. In *Evolutionary Computation (CEC), 2013 IEEE Congress on* (pp.
379 2337-2344). IEEE.

380 Zheng, Z.; Tokunaga, T. K.; Wan, J. Influence of calcium carbonate on U (VI) sorption to soils.
381 *Environmental science & technology*, **2003**, 37. Jg., Nr. 24, S. 5603-5608.